Reversible and Irreversible Coiled Coils in the Stalk Domain of ncd Motor Protein

Tsukasa Makino,[‡] Hisayuki Morii,[§] Takashi Shimizu,[§] Fumio Arisaka,[||] Yusuke Kato,[‡] Koji Nagata,[‡] and Masaru Tanokura*[,‡]

Department of Applied Biological Chemistry, Graduate School of Agricultural and Life Sciences, The University of Tokyo, 1-1-1 Yayoi, Bunkyo-ku, Tokyo 113-8657, Japan, Institute for Biological Resources and Functions, National Institute of Advanced Industrial Science and Technology (AIST), 1-1-1 Higashi, AIST-C6, Tsukuba, Ibaraqi 305-8566, Japan, and Graduate School of Bioscience and Biotechnology, Tokyo Institute of Technology, 4259 Nagatsuta, Midori-ku, Yokohama 226-8510, Japan

Received February 9, 2007; Revised Manuscript Received April 28, 2007

ABSTRACT: Ncd is a microtubule minus end-directed motor protein from *Drosophila*, a member of the kinesin-14 family, and an essential protein in mitosis and meiosis. Full-length ncd exists as a dimer via the formation of an α-helical coiled coil in its central stalk domain (P192−R346), which is thought to be one of the key regions for its motility. In our previous studies, however, none of the various synthetic polypeptide fragments (up to 46 residues) from the stalk domain formed a coiled coil. Herein, we have investigated the structural properties of the full-length ncd stalk domain using recombinant polypeptides together with shorter segments. These new fragments did form coiled coils as verified by far-UV circular dichroism (CD) spectroscopy and analytical ultracentrifugation, suggesting that a certain length of polypeptide would be required for dimer formation. Moreover, deletion mapping revealed that the cooperativity among the neighboring subdomains in the stalk domain is required for formation of the coiled coil. Interestingly, the intact stalk domain segments showed three-state transition in thermal unfolding measurements with CD, indicating the presence of two regions: (i) a coiled-coil region (P227−R306) that exhibits reversible denaturation at a lower temperature (20−30 °C) and (ii) a more rigid coiled-coil region (T307−E334) that exhibits irreversible denaturation at a high temperature (ca. 60 °C). These results imply that the N-terminal region of the stalk domain might be able to adopt both a coiled-coil conformation and a dissociated one, which might be relevant to the functions of ncd.

The kinesin superfamily consists of 14 subfamilies and other orphan kinesins. The product of the non-claret disjunctional gene of *Drosophila*, ncd, belongs to the kinesin-14 subfamily (C-terminal kinesin) and is a microtubule minus end-directed motor protein that also functions in early mitosis (*1*−*3*). Ncd is localized to spindles in meiotic oocytes and has been proposed to play an essential role, organizing the ends of spindle microtubules into poles (*4*). Ncd-specific mutation in oocytes causes highly abnormal multipolar spindles, or spindles with diffused poles, consistent with this hypothesis (*5*).

Generally, a kinesin protein has a motor domain consisting of ∼350 amino acid residues, which interacts with microtubules in a MgATP-dependent manner, an α-helical coiled coil in the middle called the stalk domain, and a tail that is thought to bind to its cargoes (*6*). In the case of ncd, the N-terminal domain (M1−A191) is the tail which is thought to bind to its cargo, i.e., microtubules, in a MgATP-independent manner (*7*), and the C-terminal domain (G347−K700) is the motor domain (*1*, *2*, *8*). The three-dimensional structure of the motor domain of ncd is very similar to that of HsKHC[1] (*9*, *10*). The region between the two (P192−R346) is the stalk domain with amphipathic heptad repeats (*7*, *11*), thought to form an α-helical coiled coil to induce protein dimerization. In fact, ultracentrifugation analysis and electron microscopic observation have shown that intact ncd and its N-terminal deletion mutants [e.g., MC5 (A295−K700)] are dimeric (*7*, *12*, *13*). In addition, X-ray crystallographic analysis of a truncated but motile ncd construct (E281−K700, PDB entry 2NCD) has confirmed that the molecules are also dimeric and that the region extending from the motor domain (L303−R346) is likely to form a two-stranded α-helical coiled coil (*14*). On the other hand, ncd constructs with further N-terminal truncation such as MC6 (M333−K700) lost the ability to form dimers and did not exhibit motility (*7*). These data suggest that the motile activity of ncd would require a dimeric structure. Near-wild-type rates of microtubule sliding occurred with a truncated stalk domain and only one head (*26*), indicating that microtubule sliding requires both strands of the ncd "neck region" but not both motor domains. On this basis, Endres et al. suggested a lever-arm model for the ncd power stroke, in which the coiled-coil stalk moved through a substantial

* To whom correspondence should be addressed. Phone: (+81)-3-5841-5165. Fax: (+81)-3-5841-8023. E-mail: amtanok@mail.ecc.u-tokyo.ac.jp.

[‡] The University of Tokyo.

[§] National Institute of Advanced Industrial Science and Technology.

[||] Tokyo Institute of Technology.

[1] Abbreviations: HsKHC, *Homo sapiens* kinesin heavy chain; TFA, trifluoroacetic acid; EGTA, *O*,*O*′-bis(2-aminoethyl) ethylene glycol-*N*,*N*,*N*′,*N*′-tetraacetic acid; CD, circular dichroism; ESI-MS, electrospray ionization mass spectroscopy; DTT, 1,4-dithiothreitol; PCR, polymerase chain reaction; PDB, Protein Data Bank; Mops, 3-morpholinopropanesulfonic acid; cryo-EM, cryoelectron microscopy; MT, microtubule; IPTG, isopropyl β-D-thiogalactopyranoside.

10.1021/bi700291a CCC: $37.00
Published on Web 07/27/2007

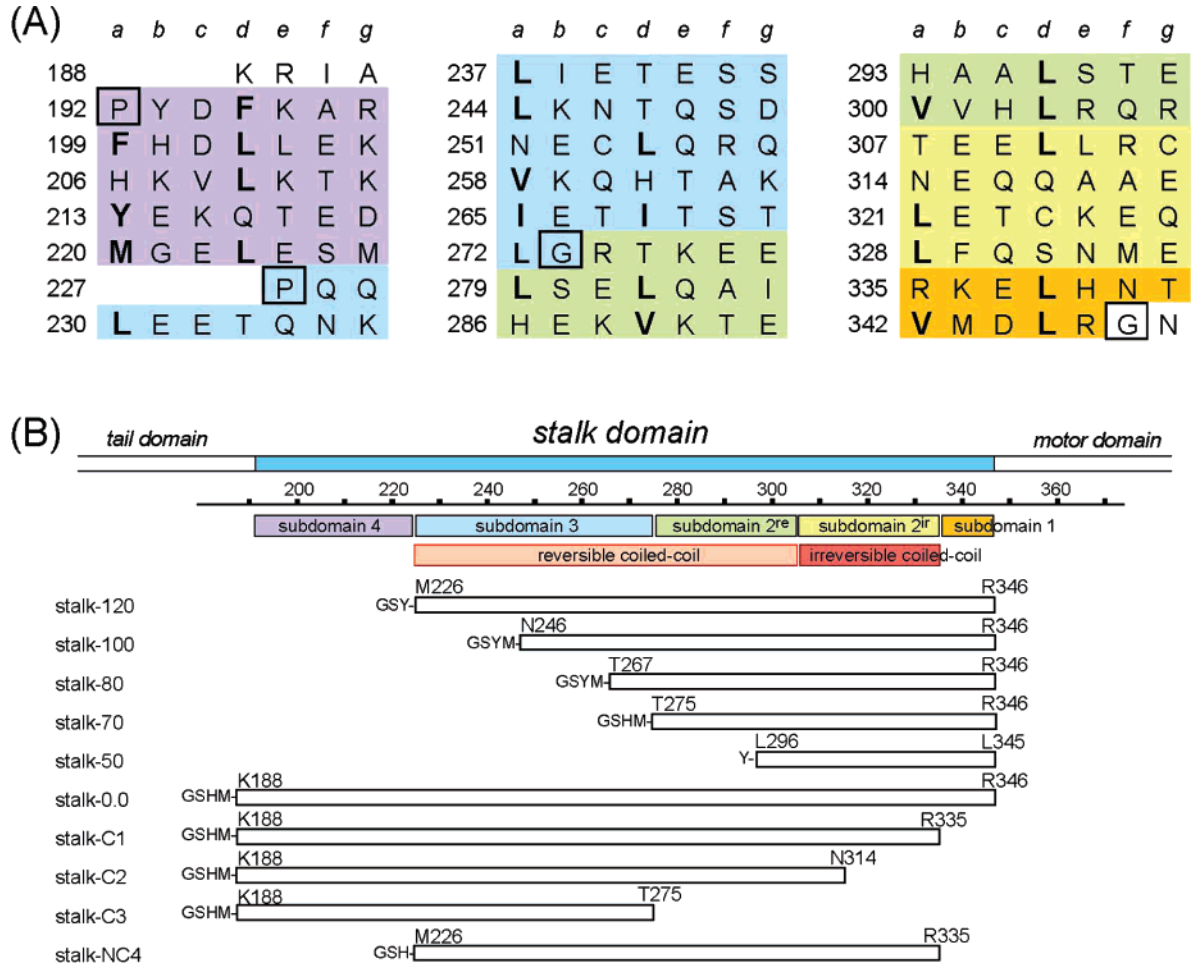

FIGURE 1: Design and preparation of N- and C-terminal deletion constructs from the ncd stalk domain. (A) Amino acid sequence of the ncd stalk domain. Heptad repeats are assigned according to the Amphisearch algorithm (*11*) and are shown in columns of seven amino acid residues denoted *a*−*g*. Hydrophobic residues at heptad positions *a* and *d* are shown with bold type. The glycine and proline residues that may break the α-helical structure are denoted with boxes. Subdomains, identified previously (*11*) and in this work, are separated by color, purple, light blue, light green, yellow, and orange, as shown in panel B. (B) Schematic representation of the ncd stalk domain and various segments used in this study. The ncd polypeptide consists of three parts: the N-terminal tail domain (M1−A191), the stalk domain in the middle (P192−R346), and the C-terminal motor domain (G347−K700). We prepared a series of stalk segments (stalk-120, -100, -80, -70, -50, -0.0, -C1, -C2, -C3, and -NC4) whose starting and ending amino acids are indicated. Polypeptide chain segments obtained from the pET28a plasmid contained three additional residues, GlySerHis, or four residues, GlySerHisMet, at their N-termini that are not part of the ncd sequence. For stalk-120, -100, and -80, on the other hand, the histidine at the additional N-terminal sequence was mutated into a tyrosine residue for convenience in the quantification. Stalk-50 with an additional tyrosine residue at the N-terminus was chemically synthesized. The reversible coiled coil (P227−R306) and the irreversible coiled coil (T307−E334) are shown as well as subdomains, i.e., subdomain 1 (R335 and R336), subdomain 2^{ir} (T307−E334), subdomain 2^{re} (R274−R306), subdomain 3 (P227−G273), and subdomain 4 (P192−M226).

angle. In this model, the stroke size is directly related to the length of the stable coiled-coil stalk.

As for HsKHC, synthetic peptides containing the top stalk region (N332−R369) have been shown to form stable two-stranded α-helical coiled coils (*15*, *16*), which are responsible for KHC dimerization. In the case of ncd, on the other hand, although the stalk domain (P192−R346) has heptad repeats, none of the frames of the stalk peptide up to 46 residues formed coiled coils under monomer−dimer equilibrium (*11*). This previous result is perplexing, since intact ncd is dimeric, so that certain conditions necessary for dimerization may still have been cryptic. One possibility is that interaction between the motor domain and the stalk domain may be important in inducing dimerization. Another possibility is that ncd peptide segments longer than 46 amino acid residues are required for dimerization.

In this study, we prepared a series of polypeptides from the ncd stalk domain with ca. 70−160 amino acid residues, longer than those examined previously (*11*). They formed coiled-coil dimers in solution, as verified by far-UV circular dichroism (CD) spectroscopy and ultracentrifugation analyses. The results of the CD experiments on thermal denaturation were then used to analyze the thermodynamic properties of the stalk domains. It was suggested that the N-terminal region of the stalk domain can change its conformation at approximately room temperature. In contrast, a specific coiled-coil subdomain exhibiting a irreversible thermal transition was found in the C-terminal region of the stalk domain. We also report our experiments on the other possibility, on the possible importance of interactions between the stalk domain and the motor domain.

MATERIALS AND METHODS

Construction of Ncd Plasmids. The segment designs are illustrated in Figure 1. Stalk-120, -100, -80, and -70 correspond to the M226−R346, N246−R346, T267−R346,

and T275−R346 regions of ncd, respectively (Figure 1A). Stalk-0.0, -C1, -C2, -C3, and -NC4 correspond to the K188−R346, K188−R335, K188−N314, K188−T275, and M226−R335 regions, respectively. The DNA segments for stalk-120, -100, -80, and -70 were amplified with PCR from the cDNA of *Drosophila* ncd, a generous gift from Dr. Toyoshima (University of Tokyo), by pairing specific forward primers that contained an *Nde*I site, P1 (5′-GGA ATT CCA TAT GCC TCA GCA ACT GGA G-3′), P2 (5′-GGA ATT CCA TAT GAA CAC CCA GAG CGA CAA CG-3′), P3 (5′-GGA ATT CCA TAT GAC AAT CAC ATC GAC GCT GG-3′), and P4 (5′-TAG GTA CCC ATA TGA CCA AAG AGG AGC TAT CCG AGC-3′), respectively, with a reverse primer that contained a *Bam*HI site, P5 (5′-TAG GAT CCT TAT TAG CGC AGG TCC ATG ACC-3′). The DNA segments for stalk-0.0, -C1, -C2, and -C3 were also generated with PCR by pairing a forward primer that contained an *Nde*I site, P6 (5′-TAG GTA CCC ATA TGA AGC GCA TCG CTC CCT AC-3′), with specific reverse primers that contained a *Bam*HI site: P5, P7 (5′-TAG GAT CCT TAG CGC TCC ATG TTC GAC TG-3′), P8 (5′-TAG GAT CCT TAA TTG CAG CGC AGG AGT TC-3′), and P9 (5′-TAG GAT CCT TAG GTC CTG CCC AGC GTC-3′), respectively. The stalk-NC4 segment was prepared by pairing a forward P1 primer with a reverse P7 primer. Amplified DNA fragments were subcloned into pET28a (Novagen, Madison, WI) to produce N-terminally His_6-tagged fusion proteins and are termed pET28a-stalk segments in this paper.

After digestion with thrombin for the removal of the His_6 tag, an additional amino acid sequence, GSH(M), derived from pET28a remained at the N-terminus of all the constructs. For stalk-120, -100, and -80, we also prepared other constructs whose histidine residue at the sequence GSH(M) was mutated into tyrosine for convenience in the quantification by 280 nm absorption. These mutations were introduced by using Quick-Change (Stratagene, La Jolla, CA) following the manufacturer's guide.

The DNA fragment encoding R350−K700 of ncd was synthesized by PCR and cloned into the *Nde*I and *Bam*HI sites in pET26b (Novagen). The primer sequences were 5′-ATA TGC ATG CAT ATG CGG GTC TTC TGT CGA ATA CG-3′ and 5′-GCT AGC GAA TTC TTA TTA TTT ATC GAA ACT GCC GCT GTT G-3′. We designated this plasmid the pET26-ncd motor domain.

Expression and Purification of the Ncd Constructs. Plasmids with the various stalk segments were transformed into Rosetta (DE3) host cells. Transformed cells were grown at 37 °C in LB medium containing kanamycin (30 μg/mL) and chloramphenicol (34 μg/mL) in an ordinary manner, and the induction was carried out by adding IPTG with subsequent culture at 25 °C. The bacteria were harvested and frozen at −80 °C.

For the stalk segment preparation, the packed frozen cells were thawed and resuspended in binding buffer [20 mM sodium phosphate (pH 8.0), 0.5 M NaCl, 40 mM imidazole, and 1 mM DTT] and were disrupted by sonication. The product in the high-speed supernatant was adsorbed onto a Ni-Sepharose (GE-Healthcare, Uppsala, Sweden) column, and the His_6 tag of the stalk segment was removed by digestion with appropriate amounts of thrombin (Amersham Biosciences, Uppsala, Sweden) at 4 °C for 48 h. The cleaved stalk segment was eluted from the Ni-Sepharose column with binding buffer, while the His_6 tag remained on the column. Thrombin was removed with Benzamidin Sepharose (Amersham Biosciences), and the stalk segment was further purified by Q-Sepharose column chromatography. The stalk segments thus obtained, which were essentially free from contaminants as shown by SDS−PAGE, were dialyzed against a solution consisting of 20 mM sodium phosphate (pH 7.0), 0.1 M NaCl, and 1 mM 2-mercaptoethanol, concentrated by using a Vivaspin ultrafiltration spin column (Vivascience, Goettingen, Germany), frozen in liquid nitrogen, and stored at −80 °C.

The recombinant plasmid pET26b-ncd motor domain containing the truncated ncd gene for R350−K700 was transformed into BL21(DE3) host cells. The cell growth and induction conditions were the same as those described above for the stalk segment constructs. The preparation of the ncd motor domain (R350−K700) was performed essentially in the same manner that was described for a slightly different version of the ncd motor domain (R335−K700) by Sablin et al. (*10*) and by Shimizu et al. (*17*). That is, the high-speed supernatant of the harvested cells was applied to a SP-Sepharose column and then to a Q-Sepharose column. The ncd motor domain that was obtained was practically pure and was dialyzed against a solution containing 20 mM Mops-NaOH (pH 7.0), 0.1 M NaCl, 2 mM $MgCl_2$, 1 mM DTT, and 5% sucrose, concentrated to 2 mg/mL using an Apollo 20 mL concentrator (Orbital Biosciences, Topsfield, MA), and stored frozen at −80 °C.

Peptide Synthesis. The stalk-50 segment, corresponding to the L296−L345 region of ncd as shown in Figure 1, was chemically synthesized by the Fmoc solid phase method as described previously (*11*). The peptide bears an additional *N*-acetyltyrosine residue at the N-terminus for convenience in spectrophotometric quantification. The molecular weight of stalk-50 thus synthesized was found to be 6135.7 (theoretical value, 6135.8) by ESI-MS. Since the synthetic peptide might contain TFA as a salt, we carried out a gel filtration to remove possible TFA contamination as follows. The dried peptide was dissolved in 0.2 M ammonium carbonate buffer (pH 9.2) containing 2 mM DTT (A buffer) to neutralize TFA as an ammonium salt and then was passed through a Superdex 75 10/30 column (Amersham Biosciences) equilibrated with A buffer. The obtained TFA-free peptide solution was desalted in milliQ water by using a PD-10 column (Amersham Biosciences) and lyophilized.

Preparation of Tubulin. Tubulin was prepared from porcine brains by cycles of polymerization and depolymerization and by DEAE-Sephacel chromatography as described previously (*18*).

CD Spectroscopy. CD spectra of the peptides in the far-UV region (190−260 nm) were recorded on a Jasco J-820 or J-720 spectropolarimeter using cylindrical quartz cuvettes with path lengths of 0.2−10 mm. The temperature was controlled at 20 °C with a water circulation system unless noted otherwise. The spectral data were collected in a solution of 20 mM sodium phosphate (pH 7.0), 0.1 M NaCl, and 1 mM DTT. The helical contents were estimated using CONTIN (*19*). The molar ellipticities at 222 nm of the stalk segments at various concentrations of peptide were fitted to the theoretical equation (eq 1) for monomer−dimer equilibrium with the molar ellipticities for the monomer state ($[\theta]_m$) and dimer state ($[\theta]_d$)

$$[\theta] = [\theta]_d + ([\theta]_m - [\theta]_d)\left(\sqrt{1 + \frac{8C}{K_d}} - 1\right)\frac{K_d}{4C} \quad (1)$$

where K_d and C represent the dissociation constant and the peptide concentration, respectively (*15*). Temperature-scanning CD measurements were carried out with a Jasco J-720 spectropolarimeter with simultaneous monitoring of ellipticity and temperature at a heating rate of 1.0 K/min. Each stalk segment showed a three-state transition, so we analyzed the data with the equations given previously (*11*), which were derived from the comprehensive theoretical treatment (*20*).

Analytical Ultracentrifugation. Sedimentation velocity experiments were performed using an analytical ultracentrifuge, Optima XL-I or XL-A (Beckman-Coulter, Fullerton, CA), with a four-hole An60Ti or eight-hole An50Ti rotor at 20 °C (unless noted otherwise). Purified recombinant stalk segment proteins were dialyzed extensively against a solution consisting of 20 mM sodium phosphate (pH 7.0), 0.1 M NaCl, and 1 mM 2-mercaptoethanol, and the dialyzing buffer was used as an optical reference. The concentration profiles were monitored by the peptide backbone absorbance at 230 nm or tyrosine side chain absorbance at 280 nm. Sedimentation velocity data were acquired at a rotor speed 55 000 or 50 000 rpm continually or with time intervals of 7 min. The protein partial specific volumes, $\bar{\nu}$ (ν-bar), buffer densities, and viscosities at specific temperatures were calculated from amino acid sequence and buffer composition, using SEDNTERP (kindly provided by J. Philo). The data analysis was conducted with SEDFIT (http://www.analyticalultracentrifugation.com), which is based on direct modeling of the sedimentation boundary, using finite-element solutions of the Lamm equation. The obtained $c(s)$ was converted into $c(M)$, assuming that the value of the frictional ratio, f/f_0, is common to all the molecular species.

For the purpose of examining whether the ncd motor domain would affect dimerization of the stalk-50 peptide, a mixture of the motor domain and stalk-50 peptide, the motor domain alone, and stalk-50 peptide alone were separately dialyzed against a solution consisting of 20 mM Mops-NaOH (pH 7.0), 0.1 M NaCl, 2 mM $MgCl_2$, 1 mM EGTA, and 0.2 mM DTT prior to ultracentrifugation analysis. Whereas runs were carried out at 4 °C, all other conditions were the same as described above. The correction for viscosity due to the temperature difference in the solution was based on SEDNTERP (see above).

ATPase Assays. The ATPase assay was performed at 20 °C in an assay mixture consisting of 20 mM Mops-NaOH (pH 7.0), 0.1 M NaCl, 2 mM $MgCl_2$, 1 mM EGTA, 0.2 mM DTT, and 5−100 μg/mL ncd motor domain, unless otherwise described. The ATPase reaction was terminated by adding a final concentration of 0.3 M perchloric acid, and the liberated phosphate was quantitated by the modified malachite green assay (*21*). The time course of the reaction was monitored to calculate the ATPase activity.

RESULTS

CD Spectra of Stalk Segments. Previously, Chandra et al. (*8*) reported that ncd N-terminal deletion mutants having stalk domain sequences of certain lengths formed dimers as verified by analytical ultracentrifugation. X-ray crystallographic analysis also demonstrated dimeric structures of similar constructs, such as E281−K700 [PDB entry 2NCD (*14*)] and H293−K700 [PDB entry 1N6M (*22*)], both of which have stalk domains adjacent to their motor domains that form two-stranded α-helical coiled coils. On the other hand, studies on a series of synthetic 46-residue peptides spanning the entire ncd stalk domain failed to detect any ability of these peptides to form coiled-coil dimers (*11*).

In this study, we have prepared a variety of recombinant polypeptides of the ncd stalk domain with ca. 70−160 amino acid residues (Figure 1B), longer than those studied previously. Far-ultraviolet (UV) CD spectroscopy was employed to probe the secondary structure of stalk segments. At 4 °C and a total chain concentration of 20 μM, the CD spectrum of stalk-50 (L296−L345), a synthetic polypeptide, indicated a more or less random-coil pattern, as seen in Figure 2, consistent with the results reported by Ito et al. (*11*). In contrast, the N-terminal deletion recombinant stalk segments, stalk-120, -100, -80, and -70 at 2 mMr (mMr denotes total residue concentration; for example, 2 mMr stalk-120 = 16.1 μM) and 4 °C, exhibited α-helix-rich CD spectra (Figure 2A), exhibiting minima at 208 and 222 nm with a $[\theta]_{222}/[\theta]_{208}$ ratio of >1, characteristic of a coiled coil (*23*). The constructs are likely dimers at this concentration. Using CONTIN, the α-helix contents were estimated to be 74−90% (Table 1). Although we prepared the stalk-60 (K288−R346) construct, it was not expressed in *Escherichia coli*.

As for the C-terminal deletion constructs, the CD spectrum of stalk-C3 (K188−T275) at 2 mMr and 4 °C indicated a random coil, as seen in Figure 2B, while segments stalk-0.0 (K188−R346), stalk-C1 (K188−R335), and stalk-C2 (K188−N314) exhibited α-helix-rich CD spectra (Figure 2B and Table 1).

The N- and C-terminal deletion stalk segment, stalk-NC4 (M226−R335), also exhibited a completely α-helical CD spectrum (Figure 2B). However, its C-terminal extension (stalk-120, M226−R346) resulted in a reduction in α-helix content. Likewise, stalk-0.0 (K188−R346), which was 12 residues longer at the C-terminal than stalk-C1 (K188−R335), exhibited lower α-helical content. The region (R335−R346), designated herein as subdomain 1 of the stalk, would be predicted to be less able to form a coiled coil, or the propensity for coiled-coil formation in this region would be much lower.

Formation of a Coiled-Coil Dimer Verified by CD Spectroscopy and Analytical Ultracentrifugation. Stalk-120, -100, and -80 were expected to form coiled-coil dimers, since they had high α-helix contents and $[\theta]_{222}/[\theta]_{208}$ ratio(s) of >1, as described above. And indeed, as shown in Figure 3, each stalk segment exhibited a remarkable concentration dependence of the molar ellipticities at 222 nm, and the data fitted well to a monomer−dimer association model (eq 1). We estimated the dissociation constants for stalk-120, -100, and -80 to be 0.76, 2.8, and 3.3 μM, respectively. It should be noted that the molar ellipticities in the low concentration range were not around −5000, the value for a random-coil structure, but −10300, −12200, and −14100 deg cm^2 dmol^{-1}, respectively. We will present our possible interpretations of these data in the Discussion.

To confirm that the stalk segments actually formed two-stranded coiled-coil dimers, sedimentation velocity analyses were performed. The dimer contents of stalk-120, -100, and -80 at 25.4, 27.5, and 32.7 μM were 87, 83, and 86%,

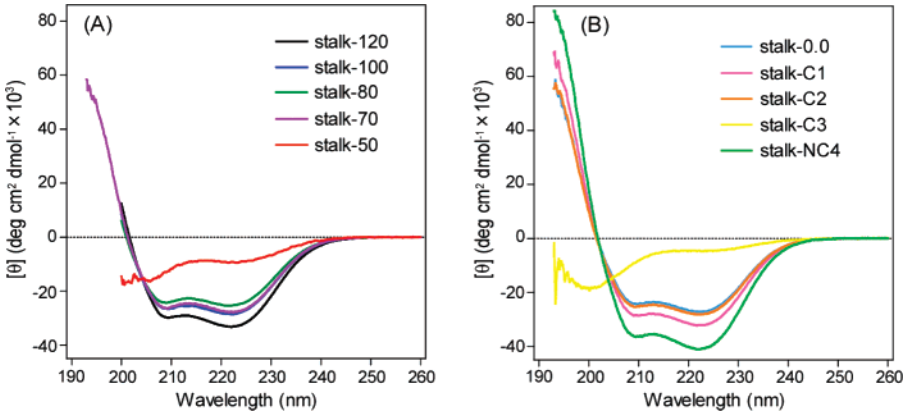

FIGURE 2: CD spectra of the stalk segments. The CD spectra of the ncd stalk domain segments studied herein are shown. Spectra in the far-UV region (190−260 nm) were recorded at 4 °C. (A) Stalk-120 (black), stalk-100 (blue), stalk-80 (green), and stalk-70 (purple) exhibited α-helical patterns while stalk-50 (red) low helicity. (B) Stalk-0.0 (light blue), stalk-C1 (pink), stalk-C2 (orange), and stalk-NC4 (light green) were α-helical, while stalk-C3 (yellow) exhibited a random-coil structure. The residue concentration of the polypeptide chain was 2 mMr for all nine segments, except for that of stalk-50 (1.02 mMr), in a solution consisting of 20 mM sodium phosphate (pH 7.0), 0.1 M NaCl, and 1 mM DTT.

Table 1: Molar Ellipticities at 222 nm, α-Helix Contents, and Molecular Weights of Ncd Stalk Segments

segment[a]	$[\theta]_{222}$[b] ($\times 10^3$ deg cm^2 dmol^{-1})	% helix[c]	molecular weight[d] (monomer)[e]
stalk-120	−33.2	90	29000 (14421)
stalk-100	−28.5	84	25200 (12224)
stalk-80	−25.3	74	21700 (9771)
stalk-70	−27.7	84	
stalk-50	−9.2	33	9100 (6135)
stalk-0.0	−27.2	76	
stalk-C1	−32.1	98	
stalk-C2	−28.1	65	
stalk-C3	−4.6	4	
stalk-NC4	−40.9	100	

[a] The amino acid sequences of the segments are shown in Figure 1. [b] The mean residue molar ellipticities at 222 nm were measured at 4 °C under the conditions described in the text. [c] The helical content (%) was estimated from the CD spectra by using CONTIN. [d] The average molecular weights of the major component peaks were derived by analytical ultracentrifugation and SEDFIT. [e] The theoretical molecular weights of the segment monomers are given.

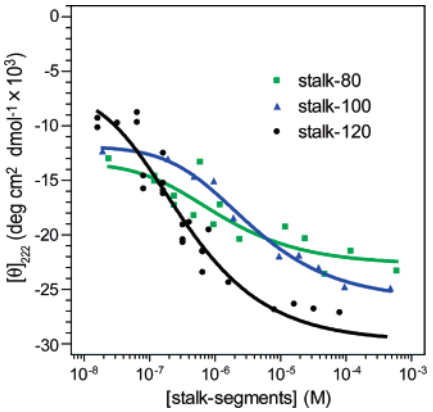

FIGURE 3: Concentration dependence of molar ellipticities at 222 nm. Molar ellipticities at 222 nm of the stalk segments at various concentrations were measured at 20 °C. Black, blue, and green traces depict the molar ellipticities of stalk-120, -100, and -80, respectively. The best-fitted curves calculated on the basis of monomer−dimer equilibrium (eq 1 in the text) are superimposed. The K_d values are 0.76, 2.8, and 3.3 μM, respectively.

respectively (Figure 4). The average molecular weights of the major component peaks derived from SEDFIT are summarized in Table 1. On the basis of the distribution of

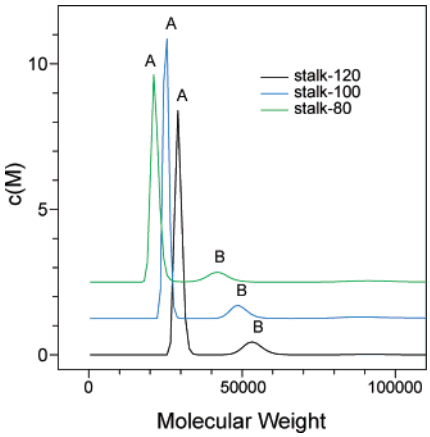

FIGURE 4: Sedimentation analysis of stalk segments. The distribution of molecular weights of stalk segments derived from analytical ultracentrifugation is shown. The experimental details are described in Materials and Methods. Sedimentation velocity data were acquired at a rotor speed 50 000 rpm and 20 °C and analyzed by SEDFIT. The initial concentrations of stalk-120, -100, and -80 were 25.4, 27.5, and 32.7 μM, respectively. Weight-average molecular weights and the content of each peak were as follows: 29 000 (87%) for A and 53 600 (11%) for B (stalk-120), 25 200 (83%) for A and 49 200 (8.7%) for B (stalk-100), and 21 700 (86%) for A and 42 000 (9.1%) for B (stalk-80).

molecular weights, it is highly probable that each of these stalk segment dimerizes through formation of a two-stranded α-helical coiled coil. We note that there were tetramers observed with contents of 11, 9, and 9% for stalk-120, -100, and -80, respectively.

Temperature Dependence of Molar Ellipticities. From the deletion mutation map (Figure 1B), the stalk domain appeared to consist of several regions that would exhibit different folding properties. To investigate the local stability of the two-stranded α-helical coiled coil, thermal unfolding profiles of various deletion mutants of the stalk domain were investigated by monitoring the CD intensity at 222 nm. As shown in Figure 5A, stalk-120 and -100 at a total residue concentration of 0.2 mMr revealed a three-state transition melting profile: a transition at 20−30 °C and another at ca. 60 °C. These two transition temperatures were common among all the stalk segments shown in Figure 5B except for stalk-C2, which exhibited an α-helix-rich CD spectrum at a

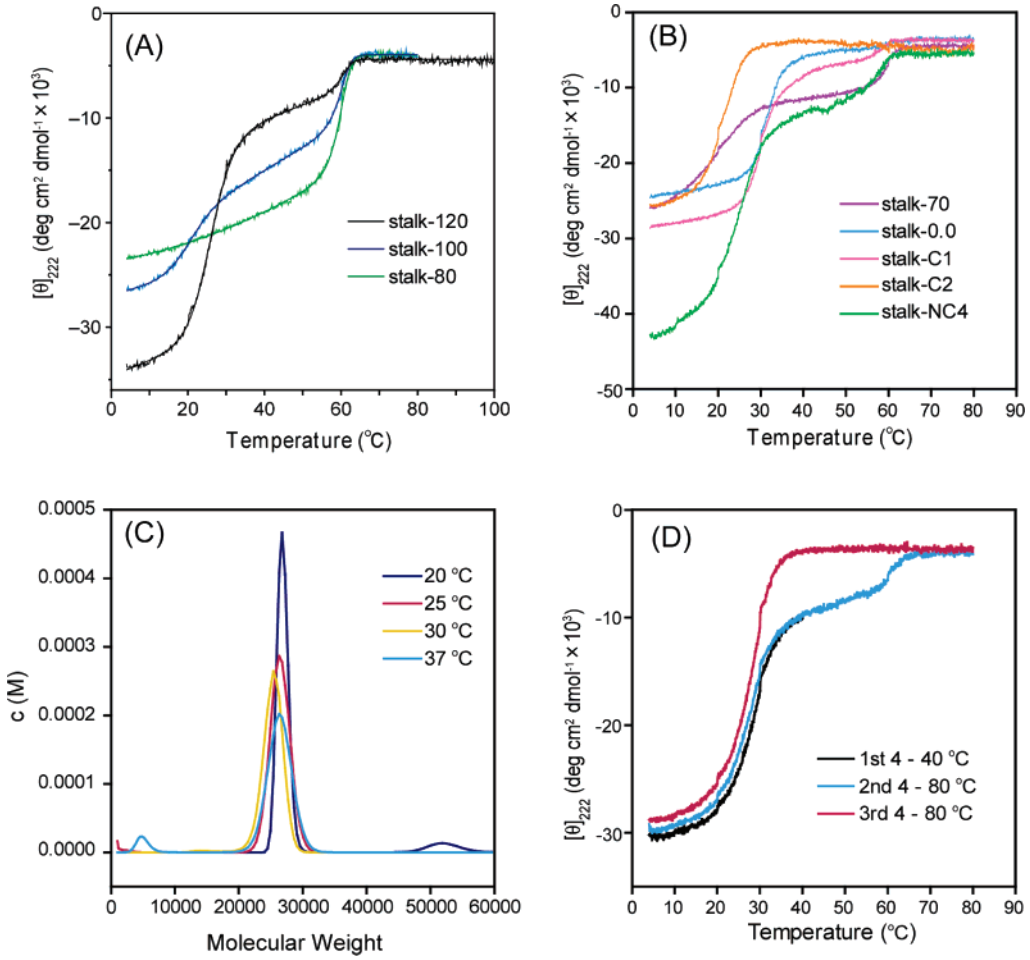

FIGURE 5: Thermal unfolding profiles monitored by CD and by analytical ultracentrifugation at various temperatures. (A and B) Thermal unfolding profiles of the stalk segments, monitored by CD molar ellipticities at 222 nm. The polypeptide residue concentrations were 0.2 mMr for all the stalk segments. (A) The profiles of stalk-120 (black), stalk-100 (blue), and stalk-80 (green) are shown. The data were analyzed with a three-state model, and the theoretical curves were superimposed. (B) The profiles of stalk-70 (purple), stalk-0.0 (light blue), stalk-C1 (magenta), stalk-C2 (orange), and stalk-4.1 (light green) are shown. Stalk-C2 exhibited a sharp single melting at 20−30 °C, while the others exhibited a three-state transition. (C) The distributions of the molecular weights of stalk-120 at various temperatures derived from analytical ultracentrifugation are shown. At each temperature, stalk-120 was mostly dimeric. (D) Multiple runs of thermal unfolding of stalk-120 monitored via molar ellipticity at 222 nm are shown. First, we measured the thermal unfolding profile from 4 to 40 °C (the first run, black line), followed by cooling to 4 °C, and then performed the second run from 4 to 80 °C (light blue line). Then the sample was cooled to 4 °C again, and the third run was performed from 4 to 80 °C. The measurement was carried out at a polypeptide residue concentration of 0.2 mMr in a solution of 20 mM sodium phosphate (pH7.0), 0.1 M NaCl, and 1 mM 2-mercaptoethanol.

low temperature (Figure 2A), with a sharp single melting at 20−30 °C but without the other at 60 °C. That the profile for stalk-C2 was so distinct from those of the other stalk segments may indicate that the difference between stalk-C1 and -C2 (N314−R335) would be indispensable for the formation of more stable coiled coils, that is, coiled coils resistant to thermal treatment up to 60 °C.

There may be two possibilities for the association state in the second phase (30−60 °C), that is, a partially unfolded dimer or partially folded monomers. To determine the state of assembly in the second phase, sedimentation velocity analysis at 20, 25, 30, or 37 °C was carried out with stalk-120 at 25.4 μM (Figure 5C). The dimer contents at these temperatures were 93, 99, 99, and 93%, respectively. At 37 °C, a temperature higher than the lower transition, the molecules were essentially dimeric. It was therefore demonstrated that stalk-120 exhibited a "folded dimer → semi-unfolded dimer → two monomers" transition when the temperature was increased from 4 to 80 °C. It should be noted that small amounts of tetramer were present at 20 °C (7.4%).

To determine whether the transitions would be reversible or irreversible, we investigated multiple runs of thermal unfolding profiles of stalk-120 monitored via the molar ellipticity at 222 nm (Figure 5D). First, we measured the thermal unfolding profile from 4 to 40 °C (the first run) followed by cooling to 4 °C and then performed the second run up to 80 °C. These two profiles were almost identical, indicating that the partial melting at a lower temperature (20−30 °C) was reversible. On the other hand, the third run from 4 to 80 °C following the second run exhibited a different profile. In the second run, there were two sharp transitions (20−30 and ca. 60 °C), but the third run revealed a single sharp melting profile; the molecules denatured completely at the 20−30 °C transition. These results indicate that the transition at a higher temperature (ca. 60 °C) is irreversible.

The thermodynamic parameters of stalk-120, -100, and -80 derived from the comprehensive theoretical treatment are summarized in Table 2. The parameters of their second transitions (T_{12} and ΔH_{12}) are apparent ones due to the lack

Table 2: Thermodynamic Parameters for Thermal Transitions of the Stalk Segments[a]

segment	K_d (μM)	T_{01} (°C)	T_{12} (at 1 M dimer) (°C)	ΔH_{01} (at T_{01}) (kJ/mol)	ΔH_{12} (at T_{12}) (kJ/mol)
stalk-120	0.76	26.0	74.3	252.1	943.1
stalk-100	2.8	19.9	74.0	214.2	910.5
stalk-80	3.3	62.4	73.5	38.7	911.3

[a] The dissociation constants (K_d) from the concentration dependence measurements using eq 1, the transition temperatures (T_{01} and T_{12} at 1 M dimer), and the van't Hoff enthalpy values (ΔH_{01} at T_{01} and ΔH_{12} at T_{12}) from the temperature dependence measurements are listed for stalk-120, -100, and -80. The basic equations for these are described in the Appendix of ref *11*.

of thermodynamic reversibility. However, these values imply the formation of a tightly folded structure with a highly cooperative nature.

Reduced Activity of the Motor Domain ATPase by the Presence of the Stalk Peptide. In the X-ray crystal structure, the C-terminal region of the stalk domain (R335−R346) forms a coiled coil, which contacts the motor domain. However, this region by itself should be less able to form a coiled coil, judging from its primary structure (*11*). In fact, stalk-0.0 (K188−R346) exhibited lower α-helicity than stalk-C1 (K188−R335), indicating that the difference, R335−R346, would not form an α-helical coiled coil when the K188−R346 region was separated from the motor domain. In addition, the stalk-50 peptide (L296−L345) was shown to be monomeric, whereas MC5 (H295−K700), an N-terminal deletion mutant of ncd with the motor domain, was dimeric. This would imply that the dimerization of the C-terminal region of the stalk domain would be triggered by contacts with the motor domain. Therefore, we prepared a stalk peptide (stalk-50, L296−L345) and a motor domain construct (R350−K700) separately and investigated whether the state of assembly of stalk-50 would be influenced by the presence of the motor domain and whether the ATPase activity of the motor domain would be affected by the presence of stalk-50.

The sedimentation velocity analysis of the 8 μM ncd motor domain or 80 μM stalk-50 peptide showed a single peak with a sedimentation coefficient of 2.33 or 0.61 S, respectively. On the other hand, 4 μM ncd motor domain in the presence of 40 μM stalk-50 showed two peaks of 0.60 and 2.27 S, but there were no other peaks with different sedimentation coefficients (data not shown). This indicates that the dimerization of the peptide corresponding to the C-terminal region of the stalk domain would not take place just as a result of mixing with the motor domain. Alternatively, the interaction might be too weak for detection by analytical centrifugation.

We assessed the influence of the stalk peptide on the microtubule-stimulated ATP hydrolytic activity of the motor domain. The ATPase activities of the 0.1 μM ncd motor domain with 1.0 mg/mL paclitaxel-polymerized tubulin were reduced to some degree via addition of 0.1−1 mM stalk-50 peptide. Sigmoidal curve fitting revealed that the concentration of the stalk-50 peptide for 50% reduction was ca. 1 mM. We next investigated the microtubule concentration dependence of the ATPase activity of the motor domain. The ATPase activities of the motor domain at a saturating concentration of microtubules with and without 2.9 mM stalk-50 were 3.9 and 5.3 s^{-1}, respectively, and the microtubule concentrations for the half-maximal ATPase activity were 0.39 and 0.33 μM, respectively (Figure 6).

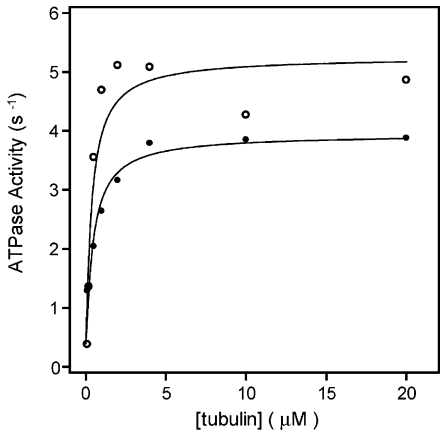

FIGURE 6: ATPase activities of the ncd motor domain with or without the stalk-50 peptide in the presence of various concentrations of paclitaxel-polymerized tubulin. The ATPase assay was carried out at 25 °C in a solution of 20 mM Mops-NaOH (pH 7.0), 25 mM NaCl, 2 mM $MgCl_2$, 1 mM EGTA, 0.2 mM DTT, 0.5 mM ATP, various concentrations of paclitaxel-polymerized tubulin, and 0.02 μM ncd motor domain (○) alone or 0.02 μM ncd motor domain in the presence of 1.92 mM stalk-50 (●). The solid lines indicate calculated hyperbolae with maximum rates of 5.3 and 3.9 s^{-1}, respectively. The half-maximal stimulations were observed at 0.33 and 0.39 μM paclitaxel-polymerized tubulin, respectively.

DISCUSSION

Interaction between Stalk Subdomain 1 and the Motor Domain. An ncd construct, MC5 (H295−K700), whose stalk domain consists of 52 residues (H295−R346), has been shown to exist as a dimer on the basis of analytical ultracentrifugation measurements (*7*). However, the corresponding peptide, stalk-50 (L296−L345), is deficient in its ability to form a dimer (Table 1). In addition, even in coiled-coil-forming stalk peptides such as stalk-120 and stalk-0.0, the region (R335−R346) seems to lack α-helicity. On the other hand, deletion of a major part of the stalk domain makes the protein monomeric as found for MC6 (M333−K700). These results suggest that formation of a coiled coil of subdomain 1 (R335−R346) at the C-terminal part of the stalk domain is largely supported by the connection with both subdomains 3 and 2 (see Figure 1) which are more likely to form a coiled coil, as well as by interaction with the motor domain.

In the motor domain ATPase assay, stalk-50, a C-terminal stalk domain peptide, reduced the ATPase activity, but only at concentrations as high as 0.1−2.0 mM (Figure 6). This means that the interaction between the motor domain and the isolated stalk peptide is rather weak and that there may be interactions distinct from that seen in the intact ncd. Together with the ultracentrifugation analysis (Figure 4), this finding suggests that the covalent linkage between the motor domain and the stalk domain is indispensable for the structure and function of ncd.

Subdomain 1 (R335−R346), also termed the "neck region" (*14*), is highly conserved in terms of amino acid sequence among the kinesin-14 subfamily members, including yeast Kar3. Most interestingly, this neck region is thought to play an important role in generating movement and in determining directionality (*24*). Ternary cooperativity among major stalk

domains (subdomains 3 and 2), subdomain 1, and the motor domain is likely to be essential for the functional structure of the ncd motor protein.

Irreversible Coiled-Coil Structure in the Stalk Domain. Many of the stalk segments examined herein exhibited two sharp transitions at 20−30 and ∼60 °C over the course of thermal unfolding (Figure 5A,B). Multiple runs of thermal unfolding measurements with stalk-120 revealed that transitions at a low temperature and at a higher one are reversible and irreversible, respectively (Figure 5D). Stalk-120 was confirmed to be dimeric at 37 °C, a temperature intermediate between the two values given above (Figure 5C). Therefore, the α-helical pattern of the CD spectrum at this intermediate state should originate from a partial two-stranded coiled coil. From these results, it is thought that subdomain 2 (R274−E334) consists of two regions bearing distinctive structural features, an irreversible and a reversible coiled-coil region. Stalk-C1 (K188−R335) exhibited two transitions, one reversible and one irreversible, in contrast to stalk-C2 (K188−N314), which exhibited a reversible transition only (Figure 5B), suggesting that the difference between stalk-C1 and -C2 (N314−R335) is indispensable for formation of the irreversible coiled coil.

To investigate the stabilizing factors of the coiled-coil dimer structure, we used PISA (Protein Interfaces, Surfaces and Assemblies Service) at the European Bioinformatics Institute (http://www.ebi.ac.uk/msd-srv/prot_int/pistart.html) (*25*) to assess the ncd dimer interface area and the interactions by using PDB entries 2NCD and 1N6M. At the *a* and *d* positions of the heptad repeat, not only the hydrophobic residues but also hydrophilic ones such as T307, N314, Q317, C324, S331, and R335 were found to participate in the dimer interfaces (Figure 1A). Though the existence of a single Asn residue at position *a* or *d* is known to be allowed for formation of a coiled coil, the consecutive existence of N314 and Q317 at positions *a* and *d*, respectively, seen in this case may be rare. The occurrence of six hydrophilic residues at nine *a* and *d* positions is remarkable in the region from T307 to R335. This might have special significance with respect to the irreversibility of the coiled coil, including N314−R335. Furthermore, polar residues at the *e* and *g* positions, such as E299, R304, E320, Q327, E334, and R346, should be effective for the stabilization. The extended hydrophobic part of these side chains would take part in the hydrophobic interactions in the dimer interface. In the crystal structure (PDB entry 1N6M), there are many hydrogen bonds (E299−R304′, T307−T307′, N314−Q317′, N314−C313′, Q317−Q317′, C324−K325′, S331−R335′, S331−S331′, E334−R335′, and S331−N332′) and electrostatic interactions (E299−R304′, E334−R335′, and K325−E320′). The irreversibility of this coiled coil may be attributable to these structure-specific interactions. Taking into consideration these structural data and the CD results for stalk-120 (discussed below), we identify the region (T307−E334) as subdomain 2^{ir}.

The NF56 peptide (H295−N340) (*11*) and stalk-50 (L296−L345), both of which include subdomain 2^{ir} (T307−E334), are able to form an α-helix under specific conditions with careful treatment, but otherwise, they are mostly nonhelical. Elongation by ∼20 residues at the N-terminus, i.e., stalk-70 (T275−R346), recovers the formation of a stable dimer so that formation of the coiled coil of subdomain 2^{ir} is likely to cooperate closely with that of the adjacent N-terminal region (R274−R306), which is designated herein as subdomain 2^{re}. In contrast, unfolding of these subdomains occurs independently, as determined via thermal denaturation. Among the N-terminal deletion mutants of ncd, MC5 (H295−K700), which includes the region of subdomain 2^{ir}, is dimeric and has motile activity, whereas MC6 (M333−K700) is monomeric and not motile. Interestingly, MC6 lacks most of subdomain 2^{ir}, suggesting that the irreversible coiled coil would be of primary importance for stabilization of the dimeric structure and for the motile activity of ncd.

Cooperative Nature of Reversible Coiled-Coil Regions. In thermal unfolding from 20 to 30 °C, stalk-120 (M226−R346) exhibited a remarkable transition of molar ellipticity at 222 nm from −29800 to −15600 deg cm^2 $dmol^{-1}$. However, stalk-100 (N246−R346), a shorter polypeptide, resulted in an apparently smaller change from −22300 to −17700 deg cm^2 $dmol^{-1}$. This can be interpreted as indicating that the M226−K245 and N246−G273 regions in subdomain 3 cooperate in formation of the reversible coiled coil. The helical content of stalk-120 at 4 and 58 °C, a temperature just below the irreversible transition, is estimated to be 87% (108 residues) and 23% (28 residues), respectively. Therefore, it can be concluded that subdomain 3 (P227−G273) and subdomain 2^{re} (R274−R306) of stalk-120 form reversible coiled coils and that subdomain 2^{ir} (T307−E334) forms an irreversible one.

In contrast to stalk-100 and -70, which undergo two transitions that are reversible and irreversible in nature, stalk-80 (T267−R346) is unique in exhibiting a single transition at a high temperature (60 °C) as if it consists of an irreversible coiled coil only (Figure 5A). The eight-residue segment (T267−R274), the difference between stalk-80 and stalk-70, may disturb the formation of a coiled coil of subdomain 2^{re} and bring about a cooperative unfolding of the rest of the coiled coil of subdomain 2^{re} and subdomain 2^{ir}. Thus, the cooperative nature between subdomains over the course of formation and unfolding of coiled coils seems sensitive to the state of their respective neighbors.

Stalk-0.0 (K188−R346), the entire stalk, formed a coiled coil. Deletion of 32 residues from its C-terminus did not affect the ability to form a reversible coiled coil which was found for stalk-C2 (K188−N314), although the ability to form an irreversible one was lost. On the other hand, further deletion of C-terminal residues, resulting in formation of stalk-C3 (K188−T275), caused a significant decrease in its ability to form a coiled coil and resulted in a random-coil structure. However, since the difference between stalk-C2 and stalk-C3 (K276−N314) has little ability to form a coiled coil independently (*11*), cooperativity between subdomain 2^{re} (T275−R306) and subdomain 3 (P227−R274) should be indispensable for formation of a coiled coil of both (Figure 1).

Coiled Coil Persisting Even at Low Concentrations. Concentration-dependent changes in the molar ellipticities were observed for stalk-120, -100, and -80, which could be interpreted as representing a monomer−dimer equilibrium, as described above. However, the molar ellipticities in the low concentration range (∼10^{-8} M) were not around −5000, the value for a random coil as observed in the thermal transition (Figure 5A,D), but rather ranged from −10000 to −14000 deg cm^2 $dmol^{-1}$ (Figure 3). These values suggest

that some α-helical structures persist even at very low concentrations. This may be attributed to the high stability of the coiled coil formed by subdomain 2^{ir} in comparison with that of the other subdomains. It is likely that some portions of dimeric molecular species undergo a slow conversion to monomeric ones during the course of dilution, perhaps due to a high energy barrier. Though the thermodynamic behavior of subdomain 2^{ir} is not fully clear, its specific features might also be responsible for the strange-looking thermal transition of the third run in Figure 5D.

Possible Roles of the Stalk in Motor Function. So far, hypotheses about ncd motility have been based on crystallographic and cryo-EM studies. Herein, by taking our findings for the ncd stalk domain into consideration, we can propose a model that involves the role of the stalk. The model is constituted by the representative three states for ncd: the MT-ncd nucleotide-free (NF) state, MT-ncd ATP (AB) state, and unbound (UB) state (*26*). In Figure 7, two MTs with different roles, i.e., a cargo-MT and rail-MT, are illustrated with some ncd molecules forming a bridge between them.

First, in the NF state, the specific binding of the motor domain onto a rail-MT and the symmetric ncd dimer with a sandwiched stalk, i.e., subdomain 1, fix the direction of the coiled coil of the stalk. Since the angle of elevation for the stalk is moderately low (NF in Figure 7A), the contact point (CP) of ncd with a cargo-MT is distant from the motor domain (MD) on the horizontal axis along a rail-MT. Endres et al. (*26*) reported that the length of the rigid stalk correlates with the gliding velocity. The rigidity should originate from the straight coiled coil of P227−R346 formed by subdomains 3, 2^{re}, 2^{ir}, and 1, because these not only have in-phase heptad repeats but also cooperate in forming coiled coils, as revealed in this work. Second, binding of ATP to the MT-bound motor, which induces the change in the interaction between subdomain 1 and the MT-bound motor (from NF to AB in Figure 7A), permits rotational Brownian movement of the stalk and MT-unbound motor around G347 as a pivot (*22*, *26*, *27*) to produce a so-called "power stroke" to drive cargo-MT (*28*). The effectiveness of this movement may also be supported by the rigidity of the stalk. Third, following the hydrolysis of ATP and release of phosphate (*26*), the motor departs from the rail-MT (from AB to UBs in Figure 7A) (*29*). In the UB state, ncd would undergo Brownian movement around the contact point with the cargo-MT (UB-1, UB-2, and UB-3). When the rigid stalk happens to take an appropriate orientation similar to the NF state like UB-3 does during this random movement, the motor could re-bind to the rail-MT and thereby release the bound ADP.

We show herein that subdomains 3 and 2^{re} have the potential to take two conformations, i.e., a coiled-coil form and a dissociated form, at ∼25−30 °C. This temperature is comparable to that in the natural environment of *Drosophila*, implying that the transition between these conformations may play important roles in the biological function of ncd. It is known that at least several ncd molecules on a rail-MT are necessary to generate translocation of a cargo-MT. This means that most of the ncd molecules, e.g., NF and UB-1 as depicted in the top illustration of Figure 7B, except the molecule which is about to generate a power stroke (NF* in Figure 7B) have to be subject to the stress caused by the motion of the cargo-MT. Probable models for such passive motions are shown in Figure 7B. It is obvious that structural

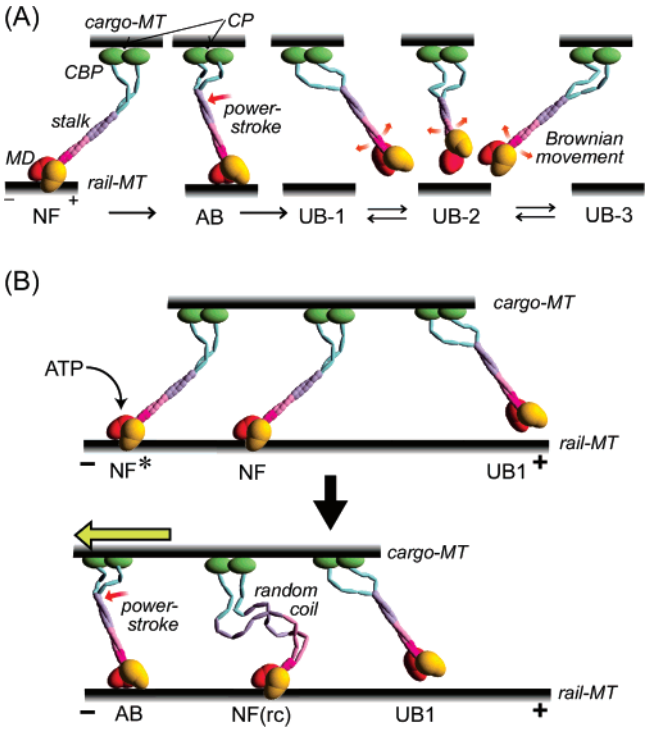

FIGURE 7: Model and possible structures of ncd during the course of translocation of the cargo microtubule. A cargo-MT and a rail-MT are shown at the top and the bottom of each ncd, respectively. The domains and/or subdomains are shown in nearly realistic, relative scale and colored as follows: a motor domain undergoing the modulation by nucleotide (red), another motor domain without binding with the rail-MT (yellow), subdomain 1 (hidden between two motor domains), subdomain 2^{ir} of the stalk (magenta), subdomain 2^{re} (pink), subdomain 3 (lavender), subdomain 4 (light blue), and a cargo-binding domain (CBP) (green). The structure of the CBP is imaginary, but its point of contact (CP) with the cargo-MT is indicated with a filled circle. (A) Possible model for the ncd movement coupled with the mechanochemical cycle of the motor domain illustrated using the proposed structures of three representative states, i.e., the nucleotide-free state (NF), the ATP-binding state (AB), and the MT-unbound state (UB) for the motor domain (MD). The UB state is defined as an ensemble of various forms in Brownian movement. Among the transient structures, UB-1, -2, and -3 shown as examples, only UB-3 is favorable for subsequent binding to the rail-MT. (B) Three ncd molecules intervening between cargo-MT and rail-MT are illustrated in the top panel. Only an ncd molecule denoted as NF* is about to bind ATP to cause a power stroke (black arrow), but the other shown as NF is not. (B) By a power stroke (red arrow), cargo-MT has just been translocated (yellow arrow) in the bottom panel. This translocation motion brings about deformation of the stalk domain of a nonworking ncd molecule in the NF state, which results in a random-coil structure as shown in NF(rc). On the other hand, the structure of the UB state does not suffer a large degree of such stress.

relaxation of the stalk is necessary so that the movement of the cargo-MT is not hindered, because the motor domain and the neck−stalk orientation are fixed in the NF state. This might be realized by the transition from a rigid coiled coil to a flexible random coil, as discussed above. On the other hand, the tightly folded coiled coil of subdomain 2^{ir} should not be relaxed so that it can contribute to the regeneration of the long coiled coil through the cooperation between subdomains in the subsequent process.

There is, however, another possible role for the unstable stalk domain. One possibility might be that it is involved in the folding of the molecule into a compact, inactive form.

To verify our stepping model shown in Figure 7B, we were required to detect the structural change at the stalk domain in the course of displacement of the cargo.

CONCLUSIONS

We have revealed (i) the formation of the long coiled coil (P227−R346) from subdomain 3 to subdomain 1 with an in-phase heptad in the ncd stalk domain, (ii) formation of the cooperative coiled coil among subdomains 3, 2^{re}, 2^{ir}, and 1 of the stalk, which might be essential in creating the rigidity and in regenerating the structure, (iii) a specific coiled-coil structure of subdomain 2^{ir} that shows an irreversible thermal denaturation, which has high thermal stability and is not readily dissociated by dilution, and (iv) the reversibility in unfolding and formation of the coiled coil in subdomains 3 and 2^{re}, which may enable the effective power stroke by preventing a possible mechanical conflict. Thus, the stalk domain of ncd is inherently equipped with an ingeniously constructed device involving reversible and irreversible subdomains, which would act in the effective translocation of cargoes by ncd. Theoretical analysis of the sequence using Amphisearch suggested that the motor proteins of the kinesin-14 subfamily may have a long coiled-coil region with at least ca. 70 residues corresponding to subdomains 3 and 2^{re} of ncd and that the N-terminus of this coiled-coil region is distant by ca. 100 residues from the pivot Gly (Gly347 for ncd). The characteristics found for the stalk of ncd might thus be conserved among the C-terminal motors of kinesin-14 subfamily members.

REFERENCES

1. Endow, S. A., Henikoff, S., and Soler-Niedziela, L. (1990) Mediation of meiotic and early mitotic chromosome segregation in *Drosophila* by a protein related to kinesin, *Nature 345*, 81−83.
2. McDonald, H. B., Stewart, R. J., and Goldstein, L. S. (1990) The kinesin-like ncd protein of *Drosophila* is a minus end-directed microtubule motor, *Cell 63*, 1159−1165.
3. Walker, R. A., Salmon, E. D., and Endow, S. A. (1990) The *Drosophila* claret segregation protein is a minus-end directed motor molecule, *Nature 347*, 780−782.
4. Hatsumi, M., and Endow, S. A. (1992) The *Drosophila* ncd microtubule motor protein is spindle-associated in meiotic and mitotic cells, *J. Cell Sci. 103* (Part 4), 1013−1020.
5. Endow, S. A., Chandra, R., Komma, D. J., Yamamoto, A. H., and Salmon, E. D. (1994) Mutants of the *Drosophila* ncd microtubule motor protein cause centrosomal and spindle pole defects in mitosis, *J. Cell Sci. 107* (Part *4*), 859−867.
6. Vale, R. D. (2003) The molecular motor toolbox for intracellular transport, *Cell 112*, 467−480.
7. Chandra, R., Salmon, E. D., Erickson, H. P., Lockhart, A., and Endow, S. A. (1993) Structural and functional domains of the *Drosophila* ncd microtubule motor protein, *J. Biol. Chem. 268*, 9005−9013.
8. Chandra, R., Endow, S. A., and Salmon, E. D. (1993) An N-terminal truncation of the ncd motor protein supports diffusional movement of microtubules in motility assays, *J. Cell Sci. 104* (Part 3), 899−906.
9. Kull, F. J., Sablin, E. P., Lau, R., Fletterick, R. J., and Vale, R. D. (1996) Crystal structure of the kinesin motor domain reveals a structural similarity to myosin, *Nature 380*, 550−555.
10. Sablin, E. P., Kull, F. J., Cooke, R., Vale, R. D., and Fletterick, R. J. (1996) Crystal structure of the motor domain of the kinesin-related motor ncd, *Nature 380*, 555−559.
11. Ito, M., Morii, H., Shimizu, T., and Tanokura, M. (2006) Coiled coil in the stalk region of ncd motor protein is nonlocally sustained, *Biochemistry 45*, 3315−3324.
12. Hirose, K., Lockhart, A., Cross, R. A., and Amos, L. A. (1995) Nucleotide-dependent angular change in kinesin motor domain bound to tubulin, *Nature 376*, 277−279.
13. Hirose, K., Lockhart, A., Cross, R. A., and Amos, L. A. (1996) Three-dimensional cryoelectron microscopy of dimeric kinesin and ncd motor domains on microtubules, *Proc. Natl. Acad. Sci. U.S.A. 93*, 9539−9544.
14. Sablin, E. P., Case, R. B., Dai, S. C., Hart, C. L., Ruby, A., Vale, R. D., and Fletterick, R. J. (1998) Direction determination in the minus-end-directed kinesin motor ncd, *Nature 395*, 813−816.
15. Morii, H., Takenawa, T., Arisaka, F., and Shimizu, T. (1997) Identification of kinesin neck region as a stable α-helical coiled coil and its thermodynamic characterization, *Biochemistry 36*, 1933−1942.
16. Tripet, B., Vale, R. D., and Hodges, R. S. (1997) Demonstration of coiled-coil interactions within the kinesin neck region using synthetic peptides. Implications for motor activity, *J. Biol. Chem. 272*, 8946−8956.
17. Shimizu, T., Sablin, E., Vale, R. D., Fletterick, R., Pechatnikova, E., and Taylor, E. W. (1995) Expression, purification, ATPase properties, and microtubule-binding properties of the ncd motor domain, *Biochemistry 34*, 13259−13266.
18. Borisy, G. G., Marcum, J. M., Olmsted, J. B., Murphy, D. B., and Johnson, K. A. (1975) Purification of tubulin and associated high molecular weight proteins from porcine brain and characterization of microtubule assembly in vitro, *Ann. N.Y. Acad. Sci. 253*, 107−132.
19. Provencher, S. W., and Glockner, J. (1981) Estimation of globular protein secondary structure from circular dichroism, *Biochemistry 20*, 33−37.
20. Kidokoro, S., Uedaira, H., and Wada, A. (1988) Determination of thermodynamic functions from scanning calorimetry data. II. For the system that includes self-dissociation/association process, *Biopolymers 27*, 271−297.
21. Kodama, T., Fukui, K., and Kometani, K. (1986) The initial phosphate burst in ATP hydrolysis by myosin and subfragment-1 as studied by a modified malachite green method for determination of inorganic phosphate, *J. Biochem. 99*, 1465−1472.
22. Yun, M., Bronner, C. E., Park, C. G., Cha, S. S., Park, H. W., and Endow, S. A. (2003) Rotation of the stalk/neck and one head in a new crystal structure of the kinesin motor protein, Ncd, *EMBO J. 22*, 5382−5389.
23. Zhou, N. E., Kay, C. M., and Hodges, R. S. (1992) Synthetic model proteins: The relative contribution of leucine residues at the nonequivalent positions of the 3−4 hydrophobic repeat to the stability of the two-stranded α-helical coiled-coil, *Biochemistry 31*, 5739−5746.
24. Endow, S. A., and Higuchi, H. (2000) A mutant of the motor protein kinesin that moves in both directions on microtubules, *Nature 406*, 913−916.
25. Krissinel, E., and Henrick, K. (2005) Detection of Protein Assemblies in Crystals, *CompLife 3695*, 163−174.
26. Endres, N. F., Yoshioka, C., Milligan, R. A., and Vale, R. D. (2006) A lever-arm rotation drives motility of the minus-end-directed kinesin Ncd, *Nature 439*, 875−878.
27. Wendt, T. G., Volkmann, N., Skiniotis, G., Goldie, K. N., Muller, J., Mandelkow, E., and Hoenger, A. (2002) Microscopic evidence for a minus-end-directed power stroke in the kinesin motor ncd, *EMBO J. 21*, 5969−5978.
28. deCastro, M. J., Fondecave, R. M., Clarke, L. A., Schmidt, C. F., and Stewart, R. J. (2000) Working strokes by single molecules of the kinesin-related microtubule motor ncd, *Nat. Cell Biol. 2*, 724−729.
29. Wendt, T., Karabay, A., Krebs, A., Gross, H., Walker, R., and Hoenger, A. (2003) A structural analysis of the interaction between ncd tail and tubulin protofilaments, *J. Mol. Biol. 333*, 541−552.

BI700291A